Available online at www.sciencedirect.com

ScienceDirect

journal homepage: www.elsevier.com/locate/burns

Point-of-care endoscopic optical coherence tomography detects changes in mucosal thickness in ARDS due to smoke inhalation and burns

Jae Hyek Choi [a,b,*], *Li-Dek Chou* [c], *Teryn R. Roberts* [a,b], *Brendan M. Beely* [a,b], *Daniel S. Wendorff* [a,b], *Mark D. Espinoza* [b], *Kyle Sieck* [a,b], *Alexander T. Dixon* [a,b], *David Burmeister* [b], *Bryan S. Jordan* [b], *Matthew Brenner* [c], *Zhongping Chen* [c], *Corina Necsoiu* [b], *Leopoldo C. Cancio* [b], *Andriy I. Batchinsky* [a,b]

[a] *The Geneva Foundation, Tacoma WA, United States*
[b] *United States Army Institute of Surgical Research, JBSA Ft. Sam Houston, TX, United States*
[c] *Beckman Laser Institute, University of California Irvine, Irvine, CA, United States*

ARTICLE INFO

Article history:
Accepted 15 October 2018

Keywords:
Acute respiratory distress syndrome
Smoke inhalation injury
Burns
Optical coherence tomography
Bronchoscopy

ABSTRACT

Background: The prevalence of acute respiratory distress syndrome (ARDS) in mechanically ventilated burn patients is 33%, with mortality varying from 11–46% depending on ARDS severity. Despite the new Berlin definition for ARDS, prompt bedside diagnosis is lacking. We developed and tested a bedside technique of fiberoptic-bronchoscopy-based optical coherence tomography (OCT) measurement of airway mucosal thickness (MT) for diagnosis of ARDS following smoke inhalation injury (SII) and burns.

Methods: 16 female Yorkshire pigs received SII and 40% thermal burns. OCT MT and PaO_2-to-FiO_2 ratio (PFR) measurements were taken at baseline, after injury, and at 24, 48, and 72 h after injury.

Results: Injury led to thickening of MT which was sustained in animals that developed ARDS. Significant correlations were found between MT, PFR, peak inspiratory pressure (PIP), and total infused fluid volume.

Conclusions: OCT is a useful tool to quantify MT changes in the airway following SII and burns. OCT may be effective as a diagnostic tool in the early stages of SII-induced ARDS and should be tested in humans.

1. Introduction

Smoke inhalation injury (SII) is diagnosed in 10-35% of patients admitted into burn units. Of the patients with SII, almost 40% subsequently develop pneumonia [1,2]. Presence of SII increases mortality by 20% over that predicted by age and burn size alone, and by up to 60% when pneumonia is also present [1]. The prevalence of ARDS in mechanically ventilated burn patients is about 33%, with mortality varying from 11–46%

* *Corresponding author at*: United States Army Institute of Surgical Research, 3600 Rawley E. Chambers Avenue, Building 3611, Ft. Sam Houston, Texas, 78209, United States
E-mail address: jae-hyek.choi.ctr@mail.mil (J.H. Choi).
https://doi.org/10.1016/j.burns.2018.10.014
0305-4179/

depending on ARDS severity [3,4]. Despite the new Berlin definition for ARDS, which enables earlier diagnosis and interventions in ARDS [5], prompt bedside identification of SII patients at risk for ARDS is lacking. In fact, development of an early scoring system for diagnosis of inhalation injury severity is an unresolved problem in critical care [6].

Early assessment of airway damage and diagnosis of SII are important to facilitate an appropriate treatment strategy. Fiber-optic bronchoscopy (FOB) has emerged as a standard method for diagnosis of SII; however, it suffers from inherent procedural risks to the patient, clinician subjectivity, inconsistent grading of injury, and false negatives in the immediate period after injury [7–12]. Several other methods have been explored for objective diagnosis of SII, such as brush cytology and broncho-alveolar lavage (BAL) cytokine analysis [7,8,11], and computed tomography (CT) of the chest [12–15]. Histological determination of diffuse alveolar damage (DAD), while a cornerstone in post-mortem ARDS diagnosis, has no practical role in early diagnosis or management of SII because it is not available in-vivo [16,17].

Optical coherence tomography (OCT) is an in-vivo laser-based imaging tool which can provide early quantitative detection of mucosal changes following tracheobronchial injury [18–20]. We previously utilized endobronchial frequency-domain OCT to obtain real-time images for quantitative assessment of regional differences in mucosal thickness (MT) over time and compared these measurements with traditional histopathology in sheep study [20]. In that feasibility study, we concluded that OCT may be useful as adjunct to FOB, but more formal studies were needed involving other clinical markers of injury severity. The purpose of the present study was to develop an approach to objective characterization of SII severity caused by combined wood-bark SII and 40% total body surface area (TBSA) flame burns in anesthetized and mechanically ventilated swine [21–23]. We utilized real-time in-vivo OCT for bedside MT measurements and correlated our findings with PaO_2-FiO_2 ratio (PFR) [5]. We sought to simplify the technique of FOB-based OCT measurements, and introduced a methodology for real-time assessment of MT at the bedside avoiding lengthy post-processing times and making the MT data available for immediate decision-making. We also correlated MT to ventilator settings and post-mortem diffuse alveolar damage scoring for ARDS, as well as total fluid volume infused and tissue moisture content. We hypothesized that MT correlates with PFR, peak airway pressure, fluid status, and ARDS risk.

2. Materials and methods

All experiments were carried out at the U.S. Army Institute of Surgical Research (USAISR), Joint Base San Antonio, Ft. Sam Houston, Texas, and were approved by the USAISR Institutional Animal Care and Use Committee (USAISR Protocols A-13-013-TS2, A-14-001, A-16-026). The study was conducted in compliance with the Animal Welfare Act, implementing Animal Welfare Regulations, and in accordance with the principles of the *Guide for the Care and Use of Laboratory Animals*.

2.1. Experimental procedures

A convenience sample of 16 female Yorkshire pigs were selected for analysis from ongoing experiments, based on availability of OCT data. As part of the main studies, all animals received ARDS-mitigating therapy in the form of either minimally invasive extracorporeal life support (n=10) or systemic administration of stem cells (n=6). (The results of those interventions will be published separately.)

After instrumentation and line placement, all animals were transported to a procedure room for administration of SII as previously described [21–23]. Briefly, smoke cooled to room temperature by mixing with an equal volume of O_2 was administered via endotracheal tube at 30 ml/kg per smoke "breath", yielding a total of 28–30 l of smoke and causing arterial carboxyhemoglobin (COHb) levels of 80–90% at end injury. After SII, a 20% total body surface area (TBSA) third-degree flame burn was induced on each flank by a Bunsen burner (total 40% TBSA) [23]. After injury, pigs were transported to an intensive care unit (ICU), where they remained under total intravenous anesthesia (TIVA) titrated to full anesthesia and round-the-clock clinical monitoring for the duration of the study [21–23]. Airway suctioning was performed as needed based on production of secretions. FOB (Olympus BF-180 bronchoscope with 2.0 mm working channel, Olympus Medical, Center Valley, PA) was performed at baseline, immediately following injury, and at every 24-h time point for the duration of the 72-h study. FOB was performed for airway toilet and cast removal. Animals received 4 FOBs: (1) after SII and burns upon arrival in the ICU; (2) in the evening of day 1; (3) during the night of day 1 or early morning hours of day 2; and (4) 24 h after injury. Additional therapeutic FOBs were performed as needed, indicated by increasing peak airway pressures greater than 35 cm H_2O not resolved by normal tracheal suctioning. At the end of study, pigs were euthanized with an intravenous dose of veterinary euthanasia solution Fatal-Plus® (phenobarbital 390 mg/ml; propylene glycol 0.01 mg/ml; ethyl alcohol 0.29 m/ml; benzyl alcohol 0.2 mg/ml; total dose 150 mg/kg; Vortech Pharmaceuticals, Dearborn, Michigan).

2.2. Arterial blood gases

PaO_2-to-FiO_2 ratio (PFR) was calculated from arterial blood gases using an iSTAT blood analyzer (Abbott Point of Care, Princeton, NJ). PFR is calculated by dividing the partial pressure of O_2 in arterial blood (PaO_2) by the fraction of inspired O_2 (FiO_2). PFR $<$300 is one of the diagnostic criteria for ARDS according to the current consensus definition [5].

2.3. Optical coherence tomography and main measurements

OCT measurements of mucosal thickness (MT) were carried out at baseline (BL), post injury (PI) and at 24, 48, and 72 h after injury as previously described, using a long-range OCT system [20]. The OCT system, designed for imaging airways in a clinical setting, consists of a 100-kHz, 1310-nm swept laser source and a fiber-based optical interferometer. The long-coherence-length laser source allows an imaging range of 24 mm using the built-in k-clock. This enables cross-sectional

imaging of an airway with a lumen diameter of approximately 50 mm, assuming the OCT probe can be positioned in the center of the airway lumen. The imaging head of the OCT probe was rotated at 6000 rpm to achieve a frame rate of 100 frames/s (at 1000 A-lines per frame). The pull-back speed of the probe was set to 25 mm/s, to keep the frame spacing at 250 μm. This allowed for shorter image acquisition time to reduce the effect of motion artifact, while allowing enough spatial data for smoother 3-D reconstruction and analysis. To optimize imaging of smaller branches in the lower airway, the focal length of the OCT probe was reduced to increase the lateral resolution.

The OCT probe was advanced via the suction port of the bronchoscope. A series of cross-sectional airway images were obtained in a single acquisition at a standardized location: between 2–4 cm along the medial wall of the right main-stem bronchus. The total time to obtain OCT images, including placing the bronchoscope, was under 1 min with an imaging time of 20–30 s. As an immediate post processing step at the bedside, MT was obtained by first selecting the corresponding OCT images acquired and then evaluating at 3 standard locations within the recorded image. Approximately 200 linear images were used to measure mucosal layer thickness in μm at each of the 3 locations, and the mean MT was taken as the injury severity marker (Fig. 1 A).

At the same time points, PFR, peak inspiratory pressure (PIP), plateau pressure, compliance, resistance, heart rate, mean arterial pressure (MAP), and total infused volume were recorded.

2.4. *Histological injury severity assessment*

For post-mortem injury severity assessment, 1.5 × 1.5 cm lung samples were excised from the upper, middle and lower sections of both lungs. Samples were fixed in 10% normal buffered formalin for 48 h, processed, embedded in paraffin and then cut into 4-μm sections. Slides were deparaffinized in histological grade xylene and dehydrated through graded alcohols to water in preparation for staining. Histological images were obtained with 100 x and 200 x magnification using an Olympus BX53 microscope (Olympus Medical, Center Valley, PA). Diffuse alveolar damage (DAD) scores were the sum of the individual scores for fibrosis, alveolar interstitial fibrosis, alveolar protein and hemorrhage deposition, type II epithelial cell proliferation and alveolar space congestion (each on a scale of 0–4) [16,24,25].

2.5. *Tissue Moisture Content*

Tissue samples from three regions of each lung (e.g. upper, middle, and lower lobes) were used to determine the tissue moisture content (MC). Briefly, each tissue sample was weighed and homogenized. Masses of each sample, approximately 1 g each, were desiccated at 150°C (HR83 Deluxe Halogen Moisture Analyzer, Mettler Toledo, Columbus, OH). Tissue moisture content is calculated as the quotient of the difference between the wet weight and the dry weight divided by the wet weight. MC is expressed as the product of this division and 100%. MC is represented as a negative percent since it represents a quantity of water lost from the tissue. MC is calculated automatically by the HR83 Moisture Analyzer throughout the procedure according to the method established in the accompanying instructional manual [26].

2.6. *Statistical methods*

SAS version 9.4, (Cary, NC) was used for all tests. All tests were two-sided with an alpha = 0.05 for significance. First a Shapiro–Wilk test was conducted to test the distribution of the data for normality. If skewed, the data was then log transformed or the nonparametric version of the test was used. All groups were tested independently using a one-way mixed model with repeated measures and a Dunnett adjustment to test significant change from baseline. Group differences were examined using a two-way mixed model with repeated measures and a Tukey adjustment. MT, PFR, PIP and total infused volume were correlated using Pearson/Spearman method. All data are means ± standard error of the mean.

3. Results

Nearly 3072 h of ICU time were required to carry out this study. Out of the 16 animals with available OCT data, 9 developed ARDS (ARDS group) at a mean time of 50 ± 5 hours after injury. Seven animals did not develop ARDS (No ARDS group). There was a similar distribution of therapeutic interventions in both groups (3 of 6 stem-cell animals developed ARDS; 6 of 10 ECLS animals developed ARDS) (NS).

OCT led to 0 complications and was safe in all animals and at all timepoints. OCT demonstrated an increase in MT at each time point after injury for all animals (Fig. 1 B and C). In animals that developed ARDS during the experiment, the mean MT was 254.95 ± 7.88 μm at BL, 457.74 ± 11.31 μm at PI, 575.67 ± 42.67 μm at 24 h, 553.27 ± 50.15 μm at 48 h and 573.11 ± 76.50 μm at 72 h (Fig. 1 B). In the No ARDS group, MT was 263.19 ± 9.22 μm at BL, 447.38 ± 37.039 μm PI, 520.05 ± 54.52 μm at 24 h, 434.12 ± 66.71 μm at 48 h, and 377.07 ± 47.18 μm at 72 h post-injury (Fig. 1C). There were no between-group differences for MT (Table 1).

PFR, ventilatory, and cardiovascular data are presented in Table 1. We observed changes over time in most variables but no between-group differences other than PFR and PIP at 48 and 72 h. Most variables showed within-group changes over time (Table 1).

We identified significant correlations between MT and PFR, PIP, total fluid volume, and tissue moisture content which, were more pronounced in ARDS animals (Table 2). Histological assessment of changes in both groups are presented in Fig. 2 as combined injury scores. Changes were not significant. The ARDS group had a significantly higher tissue moisture content than did the No ARDS group (86.2 ± 0.6% vs. 83.1 ± 0.4%, $p < 0.05$, Fig. 3).

4. Discussion

This study utilized OCT to assess temporal changes in mucosal thickness (MT) of a convenience sample of animals subjected to wood bark smoke inhalation and 40% total body surface area

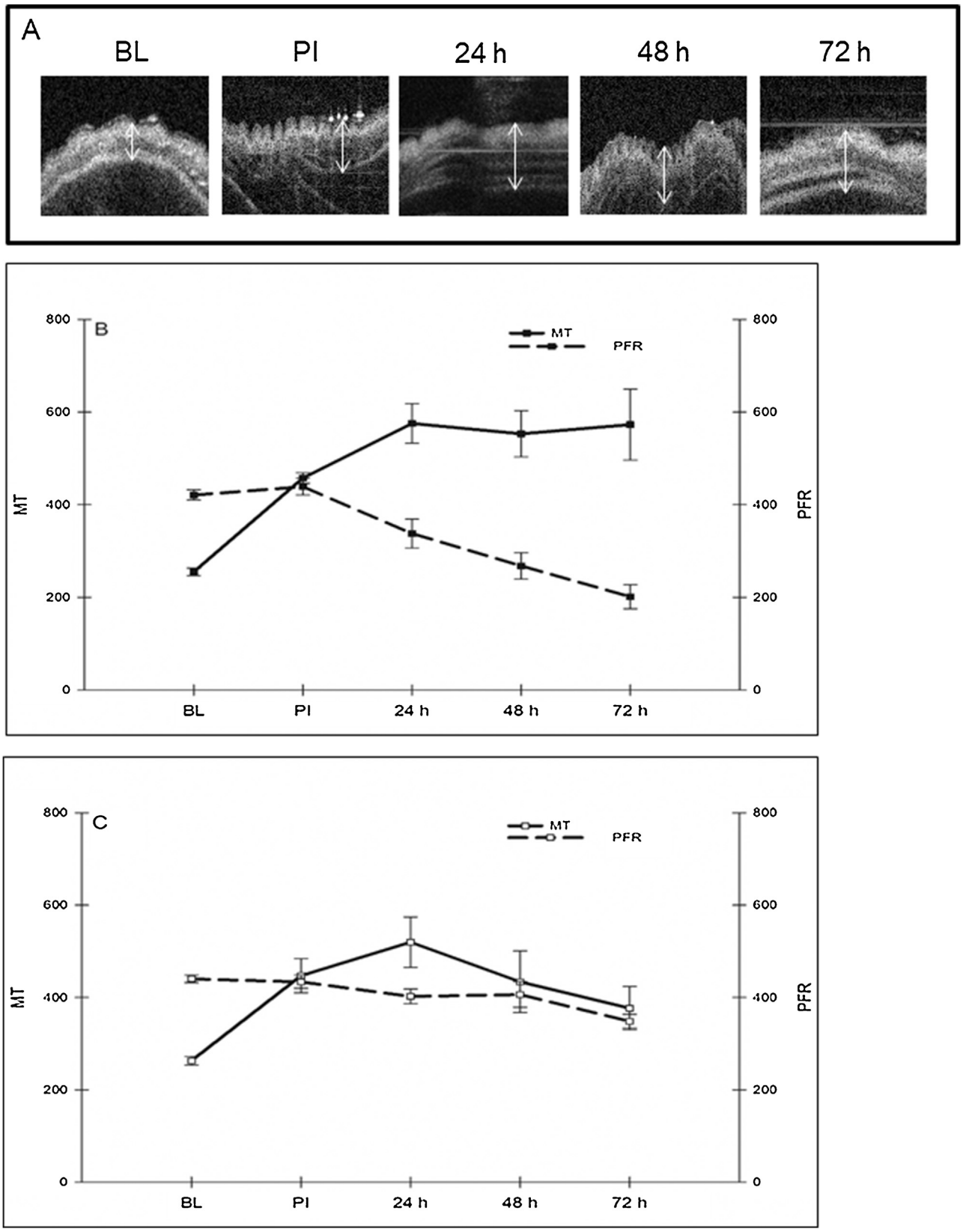

Fig. 1 – Temporal changes in Mucosal Thickness (MT) in swine subjected to smoke inhalation and burns. Measurements were performed at Baseline (BL), Post injury (PI), at 24-, 48- and 72h (24h, 48h, 72h) after injury. (A) Magnified linear OCT image showing the selected regions of interest (arrows) where MT measurements were performed in triplicates. (B) Changes in MT over time (solid line) graphed against changes in PaO_2-to-FiO_2 ratio (PFR) in animals that developed ARDS and animals that did not develop ARDS (C). Data expressed as mean ± SEM. (for significance see Table 1).

Table 1 – Changes in mucosal thickness and ventilator and hemodynamic data in ARDS and NO ARDS animals. Mucosal thickness (MT, μm); PaO_2-to-FiO_2 ratio (PFR, unitless); Peak Inspiratory Pressure (PIP, cm H_2O); Compliance (ml/cm H_2O); Resistance (cm H_2O/liter/sec), Heart rate (count per minute); mean arterial pressure (MAP, mm Hg); Total infused volume (ml). Data recorded at baseline (BL) and respective timepoints of the experiment for animals on which OCT was performed. Data are means ± standard error.

Variable	Group	Baseline	PI	24 h	48 h	72 h
MT	ARDS	254.95 ± 7.88	457.74 ± 11.31[a]	575.67 ± 42.67[a]	553.27 ± 50.15[a]	573.11 ± 76.50[a]
	No ARDS	263.19 ± 9.22	447.38 ± 37.03[b]	520.05 ± 54.52[b]	434.12 ± 66.71[b]	377.07 ± 47.18
PFR	ARDS	422 ± 11	439 ± 18	338 ± 29[a]	262 ± 29[c,a]	201 ± 26[c,a]
	No ARDS	441 ± 8	434 ± 14	403 ± 16	407 ± 28	349 ± 15[b]
Peak inspiratory pressure (cm H_2O)	ARDS	18 ± 0.5	22 ± 0.4[a]	31 ± 1.5[a]	34 ± 1.0[c,a]	40 ± 3.3[c,a]
	No ARDS	19 ± 0.6	22 ± 1.0[b]	29 ± 2.0[b]	28 ± 0.9[b]	30 ± 1.5[b]
Plateau pressure	ARDS	15 ± 0.6	18 ± 0.4[a]	23 ± 0.6[a]	25 ± 0.5[a]	31 ± 3.4
	No ARDS	16 ± 0.4	19 ± 0.6[b]	23 ± 1.5[b]	22 ± 1.3[b]	23 ± 1.4[b]
Compliance	ARDS	44 ± 3.2	38 ± 1.5	24 ± 1.6[a]	21 ± 1.8[a]	19 ± 2.5[a]
	No ARDS	45 ± 3.2	36 ± 2.2[b]	28 ± 2.5[b]	27 ± 2.9[b]	26 ± 3.0[b]
Resistance	ARDS	9 ± 2.6	10 ± 0.4	13 ± 1.8	15 ± 1.0	15 ± 2.4
	No ARDS	6 ± 0.7	11 ± 0.7[b]	13 ± 1.7[b]	11 ± 0.8[b]	13 ± 0.9[b]
Heart rate	ARDS	91 ± 3	86 ± 9	104 ± 6	118 ± 6[a]	123 ± 8
	No ARDS	95 ± 6	90 ± 16	97 ± 6.0	99 ± 8	122 ± 8
MAP	ARDS	101 ± 5	106 ± 4	92 ± 4	83 ± 7[a]	71 ± 7[a]
	No ARDS	100 ± 3	114 ± 6	100 ± 9	97 ± 9	88 ± 14
Total infused volume	ARDS	440 ± 67	1577 ± 111[a]	8613 ± 442[a]	11265 ± 228[a]	13362 ± 481[a]
	No ARDS	385 ± 46	1476 ± 72[b]	8252 ± 208[b]	11076 ± 220[b]	13522 ± 438[b]

[a] Indicates changes vs. baseline in ARDS.
[b] No ARDS animals.
[c] Indicates differences between ARDS and No ARDS groups.

burns. The main findings of the study are: (1) MT increased over time in all animals, whether they did or did not develop ARDS; an early post-injury near-doubling of MT preceded any change in the PFR. (2) MT correlated with PFR, PIP, total volume of infused fluids as well as post mortem tissue moisture content; these correlations were stronger in animals that developed ARDS. (3) MT was performed rapidly, without any complications, with results immediately available at the bedside.

OCT has been used previously to assess changes in mucosal thickness in New Zealand rabbits subjected to smoke inhalation injury [18,19]. In both studies, sustained airway swelling was documented immediately after smoke exposure and for 6 h after injury. Besides, regional differences in mucosal thickness were noted with distal airways showing more pronounced swelling [18]. Using inhaled mustard gas, Kreuter et al. demonstrated the utility of OCT in diagnosis of airway edema [27]. Although other studies were carried out using smoke in rabbits or ex-vivo applications, they largely focused on significant technological advancements of the OCT system [28–30] and less so on application of the OCT system in a translational ICU setting.

Our current data corroborate the previous findings using OCT but also refine the OCT technique for in-vivo applications and provide a blueprint for future in-vivo utilization of OCT in both animal and human studies. First, we translate previous work into a clinically relevant large animal model of ARDS due to smoke inhalation injury [21–23]. This model utilizes a human-like ICU setting and follows animals exposed to smoke inhalation and burns for up to 72 h after injury. As described in

Table 2 – Correlations between MT and PFR, PIP, Total Infused Volume and tissue moisture content (explanation in text).

Variable	Group	r-Value	p-Value
PFR	Combined	−0.3751	0.0013
	ARDS	−0.4069	0.0092
	No ARDS	−0.2304	0.2125
PIP	Combined	0.5733	<0.0001
	ARDS	0.655	<0.0001
	No ARDS	0.3134	0.0861
Total infused volume	Combined	0.53119	<0.0001
	ARDS	0.6113	<0.0001
	No ARDS	0.41452	0.0204
Wet-to-dry	Combined	0.7655	0.0005
	ARDS	0.6743	0.0464
	No ARDS	0.3055	0.5052

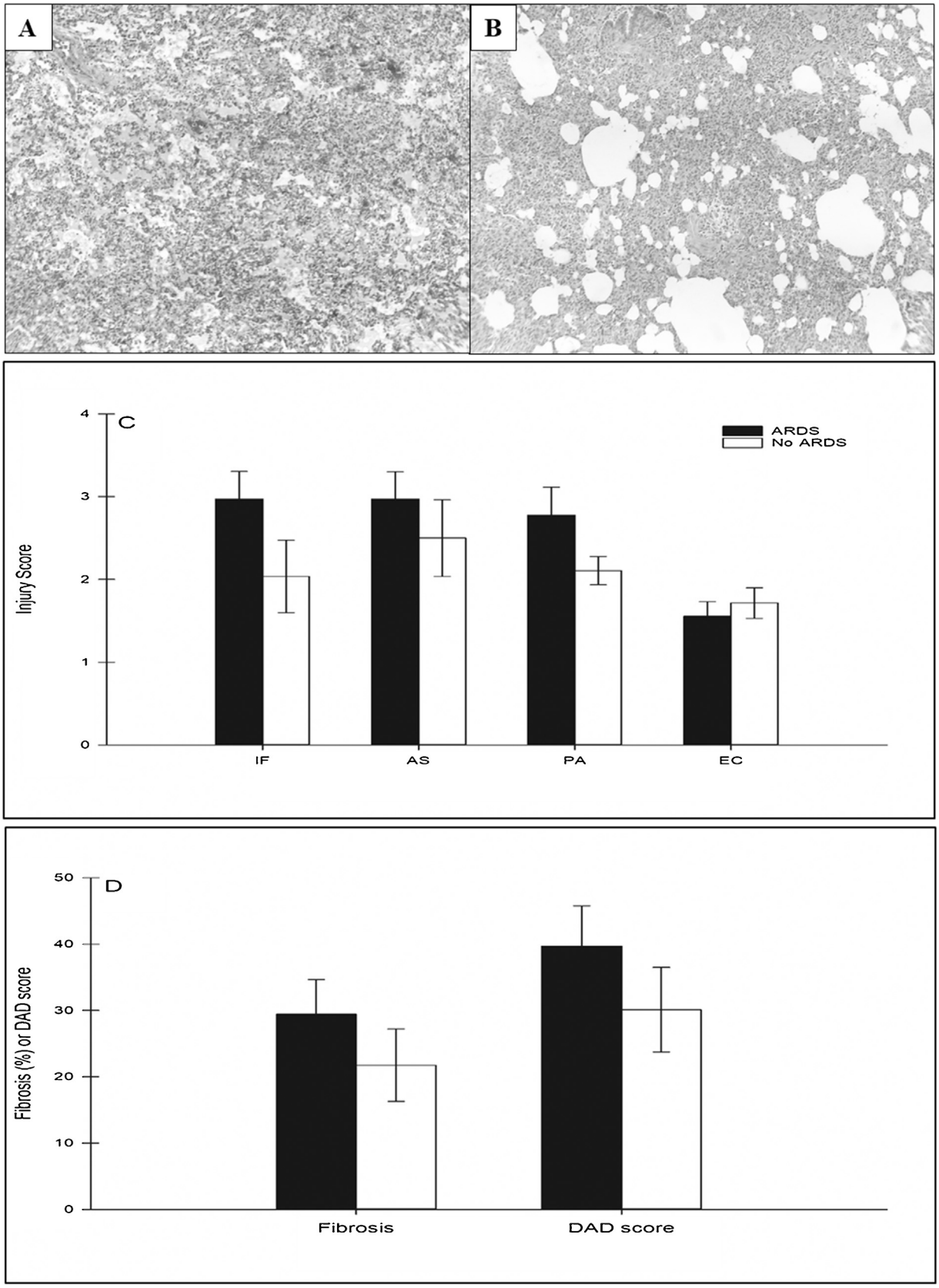

Fig. 2 – Histological Injury severity scores in ARDS vs. No ARDS animals. (A) Representative image of animal that developed ARDS (H&E, x100). (B) Representative image of animal in the No ARDS group (H&E, x20). (C) Component scores for ARDS (solid dark bars) and No ARDS (open bar) groups: interstitial fibrosis (IF), alveolar space congestion (AS), protein aggregate (PA), and alveolar epithelial type II cell proliferation (EC). Data expressed as mean ± SEM.

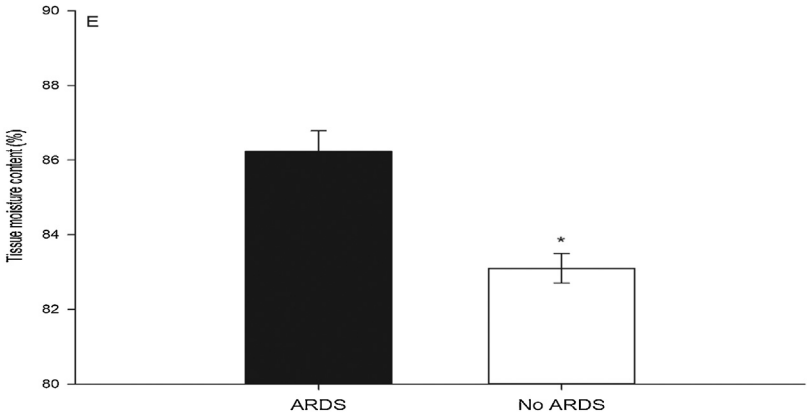

Fig. 3 – Changes in tissue moisture content in ARDS (solid dark bars) vs. No ARDS animals (open bars). Data expressed as mean ± SEM. Note significantly lower tissue moisture content in No ARDS group, $p < 0.05$).

previous iteration of this model, the usual time to development of ARDS is around 24 h after injury when no treatments are used [22]. Of note, the data presented here constituted a convenience sample from a subset of animals subjected to this model but also treated with interventions that reduced ARDS severity and delayed its occurrence. Since the mean time to ARDS was 50 h in the present study, our results need to be taken in context of a milder model, likely influenced by the treatments used. This fact is a methodological limitation, as the changes in MT may have been more pronounced if the measurements were obtained in injured but untreated animals. Nonetheless, Fig. 1 (B and C) illustrates quite clearly that MT increases as PFR decreases: signifying the potential prognostic value of OCT-derived MT at the bedside. However, these findings will have to be confirmed in pilot studies in humans to definitively confirm whether OCT is useful for ARDS diagnosis in the clinical setting.

Second, we carried out MT measurements at the bedside placing the OCT probe through the suction port of the bronchoscope. The total procedure time for bronchoscopy and OCT was usually around 1 min, making this approach feasible in the clinical ICU. No complications occurred confirming the safety of OCT. Because MT correlated highly with PFR, we propose that OCT can be a minimally invasive and highly informative diagnostic adjunct in smoke inhalation and ARDS.

Third, OCT-derived measurements, to date, involved cumbersome off-line post-processing [18,19,29-32]. All OCT data in the present study were obtained by the same operator (MD) and calculated at the bedside by the same analyst (PhD) whom averaged the regions of interest at the pre-determined location within the airway. As a rule, the numerical MT values were available within 5 min or less after bronchoscopy, turning OCT into a real-time bedside tool suitable for immediate decision making.

To reliably monitor changes in MT over time, measurement points need to be carefully selected because of the potentially large variation in tissue morphology after injury. To solve this problem, we placed the bronchoscope at the carina and oriented the camera toward the medial wall of the right main bronchus for all imaging in all animals, ensuring that the same area was imaged over time. We posit that any provider with basic bronchoscopic skills will be able to perform OCT and obtain reproducible MT measurements safely and easily. SII is traditionally diagnosed through bronchoscopy observation of findings such as carbonaceous deposits, erythema, edema, bronchorrhea, or obstruction. Efforts to quantify these findings are necessarily subjective [12,13]. In this study, we showed that high-resolution OCT has the ability to detect very small changes in tracheal mucosal thickness and is a potent tool to objectively assess airway damage.

A unique feature of this study is the longitudinal follow up of MT changes over 72 h. This work, albeit caused by severe smoke inhalation to achieve rapid ARDS development in animals, provides a reference point for future studies in the ICU setting where ARDS in humans develops over 3–5 days and where interventions such as fluid infusion over time can significantly influence MT values. In our study, MT correlated with total infused fluid volume, suggesting that MT may be also useful in assessment of impending lung damage after large infusions of fluids such as after trauma, hemorrhagic shock, and burns. This implies that patients who develop airway edema following extensive cutaneous burns and fluid resuscitation, without inhalation injury, may develop similar changes in MT and should be carefully monitored via OCT. Whether such changes would be of lesser degree than those we observed following inhalation injury will require future evaluation.

A limitation of the study is that we did not directly assess histological changes in the exact area where MT was measured by OCT. Future studies will involve direct comparison of mucosal thickness derived by OCT and histological assessment of edema at the same location. Possibly because of the mild ARDS (mean PFR >200) observed in this study, we did not see differences in DAD scores between the ARDS and No ARDS groups implying midler ARDS of treatment effects. Also, MT values did not correlate with histological lung injury scores. However, correlation of MT with tissue moisture content lends us additional confidence in the diagnostic capacity of OCT for diagnosis of lung edema.

Recent reports showed that virtual bronchoscopy and computed tomography (CT) are useful in the determination of SII severity [10,12]. We have previously shown that virtual bronchoscopy may be useful for determination of airway

narrowing in SII [12]. Yamamura et al. used CT scans to measure bronchial wall thickness and circumferential dimensions to assess mucosal swelling and airway narrowing respectively [13]. Subsequently, the same group looked at CT-scan-derived airflow narrowing as a prognostic factor in SII [10]. Both Yamamura studies showed association of CT-scan-derived metrics with ventilator days and development of pneumonia in patients [10,13]. Our current results suggest that improved OCT has the possibility to measure microscopic levels of mucosal thickness changes to better monitor the lung condition and optimize the treatment of the patient.

As we continue to search for the optimal index for assessment of airway damage and inhalation injury severity, OCT may add significant complementary information to these clinical tools. It is also possible that cumulative assessment of injury severity from all available predictors will be the best approach and may involve multifactorial predictive analytics.

5. Conclusions

These results show that OCT has the potential to detect and measure regional changes in mucosal thickness of the airway following smoke inhalation and burns. OCT may be effective as a diagnostic tool in the early stages of airway damage, smoke inhalation injury and fluid overload after burns. Further investigation is warranted to include pilot studies in humans.

Author contributions

All authors participated in study design, protocol writing, analysis of data and manuscript writing and revisions.

Acknowledgements

The authors thank the veterinary support division at the U.S. Army Institute of Surgical Research, particularly Ms. Belinda Meyers, for technical assistance with this work.

Conflict of interest

The authors declare that they have no conflict of interest.

Disclosure statement

The opinions or assertions contained herein are the private views of the authors and are not to be construed as official or as reflecting the views of the Department of the Army or the Department of Defense.

This work was supported by the U.S. Army Medical Research and Materiel Command under grant numbers W81XWH-13-2-0005, W81XWH-13-2-0006, and W81XWH-15-2-0072, and by the Air Force Office of Scientific Research under award numbers FA9550-14-1-0065 and FA9550-16-1-0369.

REFERENCES

[1] Shirani KZ, Pruitt Jr. BA, Mason Jr. AD. The influence of inhalation injury and pneumonia on burn mortality. Ann Surg 1987;205:82–7.
[2] Pruitt Jr. BA, Goodwin CW, Mason Jr. AD. Epidemiological, demographic and outcome characteristics of burn injury. Second Edition New York: WB Sanders; 2002.
[3] Dancey DR, Hayes J, Gomez M, Schouten D, Fish J, Peters W, et al. ARDS in patients with thermal injury. Intensive Care Med 1999;25:1231–6.
[4] Belenkiy SM, Buel AR, Cannon JW, Sine CR, Aden JK, Henderson JL, et al. Acute respiratory distress syndrome in wartime military burns: application of the Berlin criteria. J Trauma Acute Care Surg 2014;76:821–7.
[5] Ranieri VM, Rubenfeld GD, Thompson BT, Ferguson ND, Caldwell E, Fan E, et al. Acute respiratory distress syndrome: the Berlin definition. JAMA 2012;307:2526–33.
[6] Sison-Williamson M, Bagley A, Petuskey K, Takashiba S, Palmieri T. Analysis of upper extremity motion in children after axillary burn scar contracture release. J Burn Care Res 2009;30:1002–6.
[7] Albright JM, Davis CS, Bird MD, Ramirez L, Kim H, Burnham EL, et al. The acute pulmonary inflammatory response to the graded severity of smoke inhalation injury. Crit Care Med 2012;40:1113–21.
[8] Cindrick LL, Gore DC, Herndon DN, Traber LD, Traber DL. Bronchoscopic lavage with perfluorocarbon decreases postprocedure hypoxemia in an ovine model of smoke inhalation. J Trauma 1999;46:129–35.
[9] Pruitt Jr. BA, Cioffi WG. Diagnosis and treatment of smoke inhalation. J Intensive Care Med 1995;10:117–27.
[10] Yamamura H, Morioka T, Hagawa N, Yamamoto T, Mizobata Y. Computed tomographic assessment of airflow obstruction in smoke inhalation injury: relationship with the development of pneumonia and injury severity. Burns 2015;41:1428–34.
[11] Khoo AK, Lee ST, Poh WT. Tracheobronchial cytology in inhalation injury. J Trauma 1997;42:81–5.
[12] Kwon HP, Zanders TB, Regn DD, Burkett SE, Ward JA, Nguyen R, et al. Comparison of virtual bronchoscopy to fiber-optic bronchoscopy for assessment of inhalation injury severity. Burns 2014;40:1308–15.
[13] Yamamura H, Kaga S, Kaneda K, Mizobata Y. Chest computed tomography performed on admission helps predict the severity of smoke-inhalation injury. Crit Care 2013;17:R95.
[14] Reske A, Bak Z, Samuelsson A, Morales O, Seiwerts M, Sjoberg F. Computed tomography–a possible aid in the diagnosis of smoke inhalation injury? Acta Anaesthesiol Scand 2005;49:257–60.
[15] Park MS, Cancio LC, Batchinsky AI, McCarthy MJ, Jordan BS, Brinkley WW, et al. Assessment of severity of ovine smoke inhalation injury by analysis of computed tomographic scans. J Trauma 2003;55:417–27.
[16] Sousse LE, Herndon DN, Andersen CR, Zovath A, Finnerty CC, Mlcak RP, et al. Pulmonary histopathologic abnormalities and predictor variables in autopsies of burned pediatric patients. Burns 2015;41:519–27.
[17] Kao KC, Hu HC, Chang CH, Hung CY, Chiu LC, Li SH, et al. Diffuse alveolar damage associated mortality in selected acute respiratory distress syndrome patients with open lung biopsy. Crit Care 2015;19:228.
[18] Brenner M, Kreuter K, Ju J, Mahon S, Tseng L, Mukai D, et al. In vivo optical coherence tomography detection of differences in regional large airway smoke inhalation induced injury in a rabbit model. J Biomed Opt 2008;13:034001.
[19] Brenner M, Kreuter K, Mukai D, Burney T, Guo S, Su J, et al. Detection of acute smoke-induced airway injury in a New Zealand white rabbit model using optical coherence tomography. J Biomed Opt 2007;12:051701.

[20] Chou L, Batchinsky A, Belenkiy S, Jing J, Ramalingam T, Brenner M, et al. In vivo detection of inhalation injury in large airway using three-dimensional long-range swept-source optical coherence tomography. J Biomed Opt 2014;19:36018.
[21] Batchinsky AI. In: U.S. Army Institute of Surgical Research/ Battlefield Health and Trauma Research Institute CCCETA, editor. Extracorporeal carbon dioxide (CO2) removal for treatment of acute lung injury induced by smoke inhalation and burns in swine. .
[22] Belenkiy S, Ivey KM, Batchinsky AI, Langer T, Necsoiu C, Baker W, et al. Noninvasive carbon dioxide monitoring in a porcine model of acute lung injury due to smoke inhalation and burns. Shock 2013;39:495–500.
[23] Linden K, Scaravilli V, Kreyer SF, Belenkiy SM, Stewart IJ, Chung KK, et al. Evaluation of the cytosorb hemoadsorptive column in a pig model of severe smoke and burn injury. Shock 2015;44:487–95.
[24] Castro CY. ARDS and diffuse alveolar damage: a pathologist's perspective. Semin Thorac Cardiovasc Surg 2006;18:13–9.
[25] Thompson BT, Guerin C, Esteban A. Should ARDS be renamed diffuse alveolar damage. Intensive Care Med 2016;42:653–5.
[26] Toledo M. Operating instructions moisture analyzer HR 83 and HR 83-P. 2009:33.
[27] Kreuter KA, Mahon SB, Mukai DS, Su J, Jung WG, Narula N, et al. Detection and monitoring of early airway injury effects of half-mustard (2-chloroethylethylsulfide) exposure using high-resolution optical coherence tomography. J Biomed Opt 2009;14:044037.
[28] Tran P, Mukai DS, Brenner M, Chen Z. In vivo endoscopic optical coherence tomography using rotational MEMS probe. Opt Lett 2004;29:1236–9.
[29] Yin J, Liu G, Zhang J, Yu L, Mahon S, Mukai D, et al. In vivo early detection of smoke-induced airway injury using three-dimensional swept-source optical coherence tomography. J Biomed Opt 2009;14:060503.
[30] Su J, Zhang J, Yu L, C HG, Brenner M, Chen Z. Real-time swept source optical coherence tomography imaging of the human airway using a microelectromechanical system endoscope and digital signal processor. J Biomed Opt 2008;13:030506.
[31] Chan TM, Harn HJ, Lin HP, Chou PW, Chen JY, Ho TJ, et al. Improved human mesenchymal stem cell isolation. Cell Transplant 2014;23:399–406.
[32] Lee J, Armstrong J, Kreuter K, Tromberg BJ, Brenner M. Non-invasive in vivo diffuse optical spectroscopy monitoring of cyanide poisoning in a rabbit model. Physiol Meas 2007;28:1057–66.